A Global Spatial-Temporal Land Use Regression Model for Nitrogen Dioxide Air Pollution

Andrew Larkin[1], Susan Anenberg[2], Daniel L. Goldberg[2], Arash Mohegh[2], Michael Brauer[3,4], Perry Hystad[1]

1 Oregon State University, Corvallis, OR, USA

2 Milken Institute School of Public Health, George Washington University, Washington, DC, USA

3 Institute for Health Metrics and Evaluation, University of Washington, Seattle, WA, USA

4 University of British Columbia, Vancouver, BC, Canada

Corresponding Author: Andrew Larkin, Milam 101, Oregon State University, Corvallis, OR 97331, Telephone Number: 541-737-5413, larkinan@oregonstate.edu

TOC Art

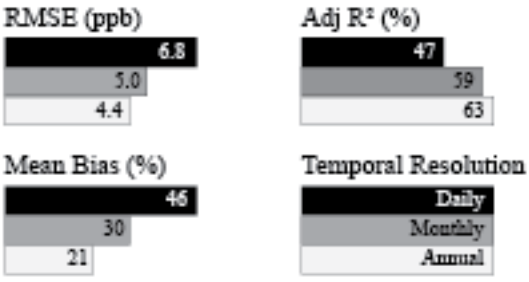

Abstract

The World Health Organization (WHO) recently reduced its health guideline for Nitrogen dioxide (NO_2) to annual and 24-hr means of 10 $\mu g/m^3$ (5.3 ppb) and 25 $\mu g/m^3$ (13.3 ppb). NO_2 is a criteria air pollutant that varies spatiotemporally at fine resolutions due to its relatively short lifetime (~hours) and current models have limited ability to capture this variation. To advance global exposure estimates, we created a daily global land use regression (LUR) model with 50 x 50 m^2 spatial resolution using 5.7 million daily air monitor averages collected from 8,250 monitor locations. In cross-validation, the model captured 47%, 59%, and 63% of daily, monthly, and annual global NO_2 variation. Daily, monthly, and annual root mean square error were 6.8, 5.0, and 4.4 ppb and absolute bias were 46%, 30%, and 21%, respectively. The final model has 11 variables, including road density and built environments with fine (30 m or less) spatial resolution and meteorological and satellite data with daily temporal resolution. Major roads and satellite-based estimates of NO_2 were consistently the strongest predictors in all regions. Daily model estimates from 2005-2019 are available and can be used for global risk assessments and health studies, particularly in countries without NO_2 monitoring.

Short synopsis: This is the first global NO_2 model with daily temporal and 50m spatial resolution, valuable for capturing NO_2 variation.

Keywords: NO_2, land use regression, global, daily

Introduction

Outdoor air pollution is an environmental health hazard. The Global Burden of Disease study estimates that outdoor air pollution was responsible for 6% (3.4 million) of global deaths in 2017 [1]. Outdoor air pollution is a combination of multiple air pollutants of concern, such as fine particulate matter, black carbon, ozone, benzene, and nitrogen dioxide (NO_2). NO_2 is a criteria air pollutant strongly associated with traffic-related air pollution and is often used in health studies as a maker of overall tailpipe emissions [2]. Studies suggest both acute and chronic exposure to ambient NO_2 is associated with adverse health outcomes. Acute ambient NO_2 exposures are associated with child asthma hospital visits [3] and adult ischemic stroke [4], while chronic NO_2 exposure is associated with increased odds of adult and childhood asthma incidence [5] and lung cancer [6]. Based on epidemiological and animal evidence, in 2021 the World Health Organization (WHO) revised its health guidelines for NO_2, reducing the annual mean NO_2 level to 10 $\mu g/m^3$ (5.3 ppb) and the 24-hr mean to 25 $\mu g/m^3$ (13.3 ppb).

Recent years have seen significant progress in advancing global NO_2 models and concomitant global NO_2 exposure estimates. Remote sensing columnar tropospheric NO_2 measurements from the TROPOspheric Monitoring Instrument (TROPOMI) are available daily at 7×3.5 km^2 resolution starting April 30, 2018 through August 5, 2019 and 5.5×3.5 km^2 thereafter [7]. The Ozone Monitoring Instrument (OMI) is the predecessor instrument to TROPOMI, launched in July 2004 and is still active [8]. While OMI reports data at a coarser resolution (24×13 km^2) than TROPOMI, the measurements are over a multi-decadal timeframe, which makes it advantageous for performing retrospective long-term trend studies [9-11], such as this one. Satellite NO_2 measurements can be reported at finer spatial resolution (~1 x 1 km^2) when aggregated to monthly, seasonal or annual timescales using a process called oversampling [12,13]. Global LUR models for annual NO_2 are available at high spatial resolutions (100m) for single snapshots in time [14], daytime and nighttime 2017 average global LUR models are available [15], and deterministic global models adjusting OMI and TROPOMI measurements with the Geos-chem chemical transport model exist at moderate spatial resolutions (~2.8km^2) [16]. However, for

health studies and burden of disease estimates (e.g. Global Burden of Disease Study [17]) that rely on retrospective exposure assessments prior to 2018, there are no global NO_2 models available with spatial resolutions < 1km and temporal resolutions < annual averages. Given that NO_2 gradients near major roads and highways rapidly fall to background levels (100-400m) and ambient NO_2 concentrations exhibit strong seasonal trends, retrospective exposure estimates require both fine spatial and temporal resolutions.

We developed a daily global NO_2 LUR model with 50 x 50 m^2 spatial resolution and coverage from 2005 to 2019. The model was trained using 5.7 million daily averages of air monitor records collected from 8,250 air monitor stations. We included a range of important datasets for prediction, including remote sensing measurements of tropospheric column NO_2 from the OMI, road networks, built up environments, and meteorological variables. This model can improve retrospective global risk estimates of NO_2 exposure and associated health burden, provide standardized NO_2 estimates for international health studies, and refine NO_2 estimates for health studies in developing countries where city- or country-specific measurements or retrospective models do not exist.

Methods

Data Collection

NO_2 Air Pollution Monitoring.

Hourly NO_2 air monitor measurements from 2005-2019 were collected from a wide range of data aggregators and environmental and regulatory agency websites (Table S1, Table 2). This includes OpenAQ (n=3.3 million daily averages) and country specific monitoring networks for the European Union (7.2 million daily averages), Japan (2.6 million daily averages), United States (2.1 million daily averages), Canada (0.8 million daily averages), Mexico (0.1 million daily averages), and South Africa (0.1 million daily averages). We did not include data that required manual data downloading since we wanted the modelling process to be repeatable and easily updated for future GBD estimates. Most regulatory NO_2 monitors use a chemiluminescence technique that suffers from a well-characterized high

bias [18,19]. This bias varies from approximately +10% to > +100% and is smallest in high-density urban (fresh emissions) and largest in rural, heavily forested regions (highly oxidized emissions) [19]. We decided not to correct for this monitor bias since most epidemiological studies are based on unadjusted regulatory monitoring data. We excluded air monitor records prior to 2005 as several predictor variables, most notably OMI, are not available prior to 2005. Daily 24-hour averages (12 am to 11pm local time) were calculated if at least 18 of the 24-hour measurements were valid. Daily averages greater than 250 ppb (above the 99.99th percentile) were excluded. Monthly averages were calculated if at least 50% of the daily averages within a month were valid. Annual averages were calculated if 50% of the daily averages within the year and two monthly averages within each quarter were valid. For duplicate air monitor records in multiple databases, validated air monitor records from regulatory agencies were kept while unofficial hourly measurements from air quality websites were discarded. The final database included 5.7 million daily air monitor averages collected from 8,250 air monitor locations.

Predictor Variables.

Predictor data derived for each monitoring state are summarized in Table 1. Data were downloaded at the temporal resolution listed in Table 1 and for each fine-scale land use characteristic, multiple buffer variables were created, ranging from 50m to 20km in radius. Buffer variables and point estimates were calculated using Python 3.8.8 scripts written for automated analysis in ArcGIS Pro 2.8.0. Python scripts are available at https://github.com/larkinandy/LUR-NO_2-Model.

Table 1. Predictor Variables Derived for 8,250 Air Monitor Locations, Ordered by Temporal Resolution Available.

Variable	Spatial Scale	Temporal Scale	Years	Unit	Source
Major Roads	na	na	2018	na	www.openstreetmap.org
Minor Roads	na	na	2018	na	www.openstreetmap.org
Residential Roads	na	na	2018	na	www.openstreetmap.org
Major Railways	na	na	2018	na	www.openstreetmap.org

Minor Railways	na	na	2018	na	www.openstreetmap.org
Water Body	30m	na	2018	indicator	developers.google.com/earth-engine/datasets/catalog/GLCF_GLS_WATER?hl=en
Elevation	30m	na	multiple years		developers.google.com/earth-engine/datasets/catalog/USGS_SRTMGL1_003?hl=en#description
Population Density	1km	five year	2005-2020	persons/km	developers.google.com/earth-engine/datasets/catalog/CIESIN_GPWv411_GPW_Population_Density?hl=en
Tree Cover	30m	five year	2005-2015	%	landsat.gsfc.nasa.gov/article/global-30m-landsat-tree-canopy-version-4-released
Power Plant Emissions	na	annual	2016	tons CO_2/year	developers.google.com/earth-engine/datasets/catalog/WRI_GPPD_power_plants
Built Environment	30m	annual	2005-2018	indicator	developers.google.com/earth-engine/datasets/catalog/Tsinghua_FROM-GLC_GAIA_v10?hl=en
NDVI	250m	monthly	2005-2019	normalized units	developers.google.com/earth-engine/datasets/catalog/MODIS_006_MOD13Q1
CEDS Sector Specific NO_2 Emissions	0.5˚	monthly	2005-2019	total mass	www.globalchange.umd.edu/ceds/ceds-cmip6-data/
Active Fires	0.1˚	daily	2005-2019	megawatts	developers.google.com/earth-engine/datasets/catalog/MODIS_006_MOD14A1?hl=en
Boundary Layer Height	31km	daily	2005-2019	m	www.ecmwf.int/en/forecasts/datasets/reanalysis-datasets/era5
OMI NO_2 column density	0.25˚	daily	2005-2019	mol/m^2	registry.opendata.aws/omi-no2-nasa/
Surface Pressure	31km	daily	2005-2019	Pa	www.ecmwf.int/en/forecasts/datasets/reanalysis-datasets/era5
Temperature	31km	daily	2005-2019	K	www.ecmwf.int/en/forecasts/datasets/reanalysis-datasets/era5
Precipitation	31km	daily	2005-2019	m	www.ecmwf.int/en/forecasts/datasets/reanalysis-datasets/era5
Downward UV Radiation	31km	daily	2005=2019	Jm^{-2}	www.ecmwf.int/en/forecasts/datasets/reanalysis-datasets/era5

The temporal scale of variable predictors varied substantially based on availability. Road and railway networks were extracted from an August 2018 snapshot of the OpenStreetMap (OSM) geodatabase. We reclassified OSM road and railway networks into the following categories: Major roads were derived from OSM motorways, motorway links, trunks, trunk links, primary and secondary roads and links. Minor roads were derived from OSM tertiary roads and tertiary road links. Residential roads were derived from OSM residential roads and residential road links. Other OSM road classifications (e.g.

service roads and bridleways) were excluded. Major railways were derived from OSM mainline railways, and minor railways were derived from OSM light rail and monorails. Other predictors were available for temporal scales of 5 years, annually, monthly, or daily for our study period of 2005-2009.

Daily temporal variables included NO_2 tropospheric column density measurements and meteorological data. Daily NO_2 tropospheric column density measurements from the Ozone Monitoring Instrument (OMI) version 4.0 [20] were downloaded from NASA. Measurements were preprocessed by NASA with a screen for snow cover, cloud fraction < 30%, and data unaffected by an instrument obstruction called the row anomaly. Monthly averages were calculated if 25% of the daily averages were valid, and annual averages were calculated if 25% of the daily averages within the year and 1 monthly average within each quarter were valid. This screening will disproportionately affect polar and cloudy regions and have no effect on areas with climatologically clear skies. For meteorology, hourly boundary layer height, precipitation, surface temperature, and near surface atmospheric pressure predictions generated by the European Centre for Medium-Range Weather Forecasts (ECMWF) Reanalysis Model v5 (ERA5) were downloaded from the ECMWF database. Daily averages (12am to 11pm local time) were calculated after adjusting for local time zones.

Statistical Analysis

Daily LUR models were developed using Lasso variable selection (glmnet package in RStudio, v. 1.4.1106), weighted by geographical and seasonal coverage. We used weights to account for the different global and season coverage of the available NO_2 monitoring data, to better model global NO_2 concentrations and predictors. Appendix Figure S1 describes the weighting method used. Parameters for Lasso variable selection include standardizing independent variables (standardization = True), selecting variables to minimize mean-squared error (type.measure='mse), and forcing the direction of variable coefficients to conform to a-priori hypotheses (lower.lim=0). The lasso model with a lambda cross-validation score of one standard deviation from the minimum cross-validation score was selected as the model of choice to favor model simplification and inference over model prediction (s=lambda.1 se). To

reduce multicollinearity, models with incremental buffer sizes of the same land use characteristics were reduced to include the smallest buffer size, if the radii of the larger buffers were within 5 times the radii of the smaller buffers. Variables were included in the final model if they were statistically significant, increased adjusted R^2 either globally or within one or more continental regions by 1 percent or more, exhibited variance inflation factors less than 5 for at least one region and less than 10 for all regions.

To evaluate the final model performance, we calculated root mean squared error (RMSE) mean absolute error (MAE), adjusted R-squared (Adj. R^2), mean percent bias (MB) and mean absolute bias (MAB) for the entire global dataset as well as within each continental region. Leave 10% out cross-validation was performed, in which 10% of the monitors from each continental region were randomly sampled into a testing dataset, with the remaining 90% combined to create the model training dataset. Cross-validation was repeated in a bootstrap fashion 10,000 times to generate cross-validation estimates of RMSE, MAE, Adj. R^2, MB, and MAB both globally and within each continental region.

In chronic health studies, exposure estimates are often aggregated to monthly or annual averages to better capture seasonal and chronic NO_2 exposure trends. To test the performance of model aggregations, we derived monthly and annual averages of daily model predictions and compared them to monthly and annual averages of air monitor measurements. We also created a separate LUR model using annual rather than daily air monitor records and predictor variables and compared the performance of the annual and daily NO_2 models in predicting annual NO_2 concentrations.

In our previous 2010-2012 model, RMSE and MB were greater in rural vs. urban areas. To test model performance across urban development levels, we identified urban development levels at air monitor locations using the Global Human Settlement layer [21] and stratified daily, monthly, and annual cross-validation by urbanicty.

All of the R scripts used to create the LUR models, perform model performance, and perform sensitivity analyses are available at https://github.com/larkinandy/LUR-NO_2-Model.

Results

Global NO_2 Database

The geographical distribution of NO_2 annual averages are shown in Figure 1. Summary statistics for daily NO_2 averages stratified by region are shown in Table 2. More than 5.7 million days of valid measurements were collected from 8,250 air monitor locations. Air monitor coverage is greatest in Asia, Europe, and North America and sparse in Oceania, South America, and Africa. Annual concentrations range from 0 to 59 ppb (mean = 11.8), while daily concentrations range from 0-249ppb (mean = 11.7). Mean daily concentration is noticeably lower in Oceania (4 ppb) in comparison to other regions (9-13 ppb). Daily standard deviation is likewise lower in Oceania (4 ppb) compared to other regions (9-11 ppb).

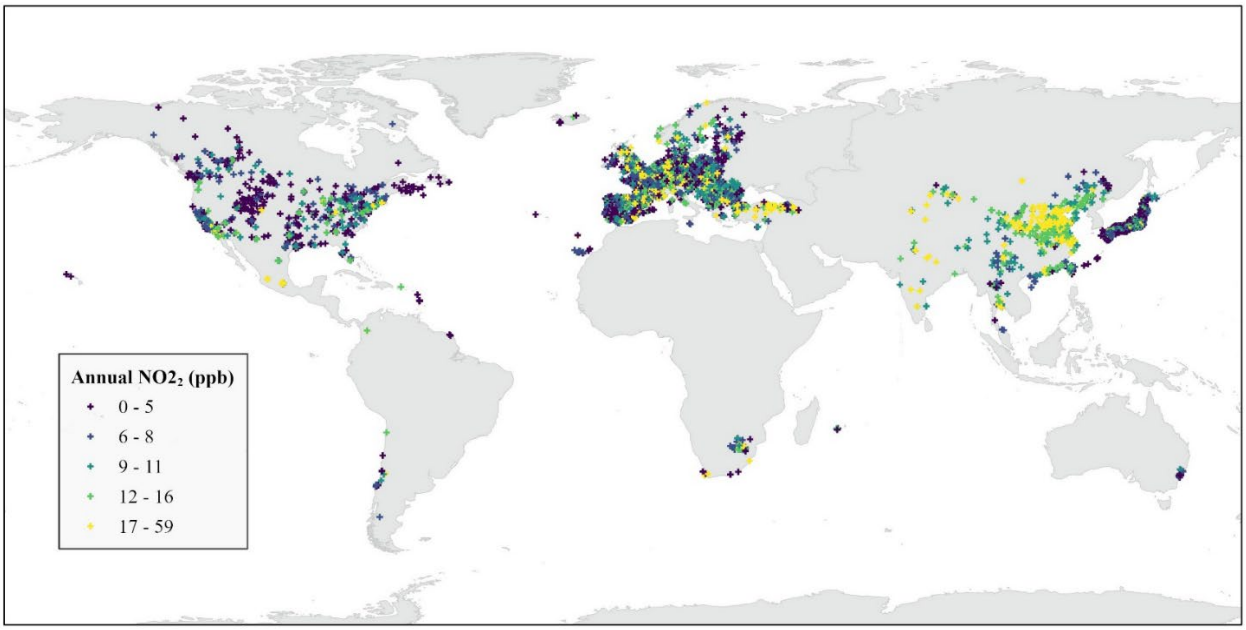

Figure 1. Global Distribution of NO_2 Air Monitor and Annual NO_2 Concentrations (2005-2019). For air monitors with multiple years of measurements the most recent annual average is shown**.**

Table 2. NO_2 Air Monitor Summary Statistics (2005-2019), Stratified by Region**.**

Region	Daily Averages (n)	Monitors (n)	Min NO_2 (ppb)	Max NO_2 (ppb)	Mean NO_2 (ppb)	SD NO_2 (ppb)	25th %	50th %	75th %	90th %
N America	1315926	1056	0	139	10	9	4	8	15	23
S America	12581	47	0	245	11	11	4	8	15	25
Europe	1922511	3475	0	224	11	9	5	9	16	23
Africa	105078	124	0	249	9	10	4	6	11	19
Asia	2343387	3522	0	241	13	10	6	11	18	26
Oceania	14674	25	0	87	4	4	2	3	5	8
Global	5714157	8250	0	249	12	9	5	9	16	24

Global LUR Model

Model Performance

Global NO_2 predictions are shown in Figure 2 for the final global LUR model. Cross-validation performance is shown in Table 3. See Figure S3 for a closer look at model predictions below 5ppb. Additional performance metrics are available in Table S5. Using 10% cross-validation, the model predicts 47% of daily, 59% of monthly, and 63% of annual global NO_2 variation. Model predictions are positively biased, with bias greatest for daily predictions (46%) and smallest for annual predictions (21%). Similarly, RMSE is greatest for daily predictions (6.8 ppb) and smallest for annual predictions (4.4 ppb). Regionally, explained variance in daily predictions ranged from 10% (Oceania) to 57% (North America). In general, model performance improved in each region when aggregating daily predictions to monthly and annual averages. Except for Oceania, annual averages of model predictions explained 49% to 66% of annual NO_2 variation within each region. Explained annual variance for Oceania is just 2% (due to limited measured NO_2 variation in our dataset).

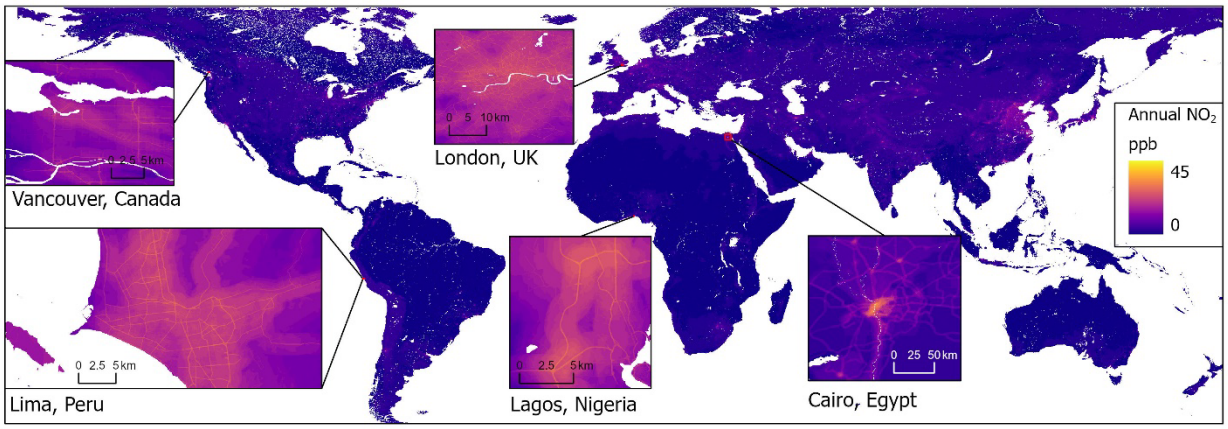

Figure 2. Global NO_2 Model Predictions for the Year 2018. Inserts of select cities for each continental region demonstrate within city variation of model predictions.

Table 3. Cross-Validation Model Performance at Predicting Daily, Monthly, and Annual NO_2 Concentrations.

	Daily			Monthly			Annual		
	RMSE (ppb)	**Adj R^2 (ppb)**	**MB (%)**	**RMSE (ppb)**	**Adj R^2 (ppb)**	**MB (%)**	**RMSE (ppb)**	**Adj R^2 (ppb)**	**MB (%)**
Global	6.8	0.47	46	5.0	0.59	30	4.4	0.63	21
Region									
N America	6.4	0.51	57	4.9	0.54	49	4.0	0.62	34
S America	6.2	0.37	55	4.4	0.50	37	3.4	0.66	28
Europe	6.4	0.45	39	4.8	0.53	26	4.3	0.56	17
Africa	6.7	0.35	54	5.1	0.39	23	3.8	0.49	22
Asia	7.3	0.40	45	5.2	0.53	24	4.6	0.54	17
Oceania	5.7	0.10	168	5.5	0.10	164	5.6	0.02	120
Global	6.8	0.47	46	5.0	0.59	30	4.4	0.63	21
Abbreviations: RMSE – root mean square error, Adj R^2 – adjusted R^2, MB – mean percent bias.									

Model Structure

Predictor variables and contributions to model performance are shown in Table 4. Predictor variables include satellite based NO_2 estimates (OMI), meteorological conditions (temperature, atmospheric pressure), land use characteristics with positive coefficients (major, minor, and residential roads, population density) and land use characteristics with negative coefficients (tree cover, water body).

The most significant variable is major roads within 50m. Buffer sizes range from 50m (major roads) to 20km (water body). Major roads and OMI each consistently explain more than 5% of the NO_2 variation both globally and within all regions. However, the importance of other model variables varied between regions. For example, built up environment explains 12% of the NO_2 variation within Africa, but only 1.6% globally. Similarly, atmospheric pressure explains 5.1% of the NO_2 variation in South America, but less than 0.1% globally.

Variables in the model with daily temporal resolution include OMI, temperature, and atmospheric pressure. The built up environment variable has annual resolution, while the tree cover and population density variables were updated every five years. Road networks and water body predictors were derived from a single time point and do not capture changes over time.

Table 4. Global LUR Model Structure.

Variable	Units	IQR	Trans-formation	Buffer Radius (km)	β	Std Err	Global %R^2 Reduction*	Regional %R^2 Reduction**
Major Roads	km^2	0.00E+00	sqrt	0.05	9.29E+00	2.85E-02	7.5	10.4
OMI	molec. /cm^3	1.80E+04	sqrt/blh	NA	1.32E-06	5.20E-07	6.2	15.2
Built Environment	%	5.10E-01	sqrt	2.5	2.90E+00	1.63E-02	1.6	11.9
Population Density	persons/ km	3.34E+01	sqrt	3	8.00E-02	1.72E-04	1.5	1.8
Tree Cover	%	2.15E+00	sqrt	10	-3.92E-01	1.75E-03	1.1	5.1
Major Roads	km^2	1.74E+00	sqrt	1.5	1.15E+00	2.47E-03	1.1	1.8
Minor Roads	km^2	3.02E-01	sqrt	0.05	1.86E+00	2.27E-02	0.9	1.9
Residential Roads	km^2	7.17E-01	sqrt	0.2	6.27E-01	6.32E-03	0.8	1.5
Water Body	%	4.13E-01	sqrt	20	-3.44E+00	1.28E-02	0.7	4.1
Temperature	K	1.14E+01	-	NA	-1.40E-01	4.50E-04	0.5	4.8
Atm Pressure	Pa	3.40E-02	ln	NA	9.53E-01	3.04E-03	0.1	5.1

*Global reduction in explained variance after removing variable from the model. **Maximum reduction in explained variance in each region after removing variable from the model. Variables are listed in order of global %R^2 reduction. All variables were statistically significant ($p < 0.001$). Abbreviations: OMI – Ozone Monitoring Instrument, Atm – atmospheric.

187 Spatial and Temporal Distribution

188 Figure 3 illustrates the different temporal predictors of the final model with January, July, and
189 annual 2011 averages for Delhi, India. Also shown in Figure 3 are the three year 2010-2012 average
190 predictions from a previously published LUR model developed with similar methodology and predictor
191 variables [13]. In general, the spatial distribution of NO_2 is similar for both monthly and annual averages.
192 Concentrations are greatest in areas with dense population density and built up environment (Eastern
193 Delhi) and alongside major road networks. While spatial patterns are consistent across the year, the
194 magnitude of predicted NO_2 concentrations differs between months and the annual average. Predicted
195 NO_2 levels are noticeably above and below the annual average in January and July, respectively, in
196 agreement with seasonal trends of NO_2 lifetime in the Northern Hemisphere [22]. In comparison to
197 2010-2012 model published by Larkin et al [13], inclusion of minor and residential roads in the present
198 model adds NO_2 traffic-related gradients outside of the dense urban core.

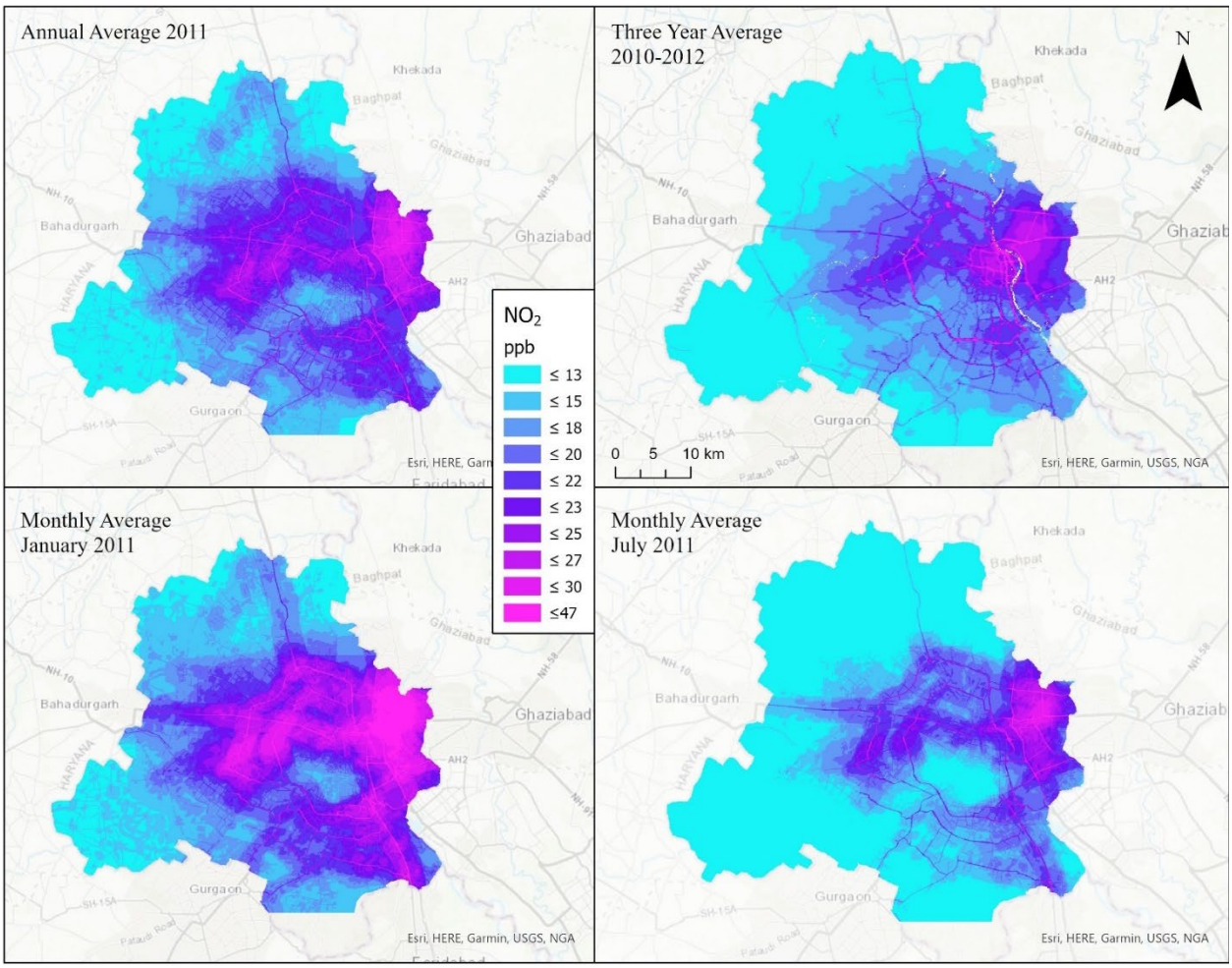

Figure 3. Comparison of NO_2 Estimates Across Delhi, India. Top Left: annual 2011 averages of daily model predictions. Bottom left and right: Average model predictions for January and July 2011, respectively. Top right: three year 2010-2012 average predictions from a previously published global NO_2 land use regression model using similar predictor variables (Larkin et al, 2017).

Sensitivity Analysis

Cross-validation performance of annual predictions derived from daily and annual NO_2 LUR models are shown in Table 5. Globally, model performances are similar. RMSE and MAE differ by 0.1 ppb, MB and MAB differ by 1 and 2%, respectively, and Adj R^2 differs by 0.02. Regionally, the daily and annual models differ the most in South America (RMSE and Adj R^2 are 1.2 ppb lower and 0.09 higher, respectively for the daily model) and Oceania (RMSE is 0.9 ppb lower for the annual model, while Adj R^2 is equal between the daily and annual models). In general, results suggest the error in

annual averages of daily model predictions does not significantly differ from predictions generated by an LUR model optimized for predicting annual concentrations.

Table 5. Cross-Validation Performance of Daily and Annual LUR Model Performances in Predicting Annual NO_2 Concentrations.

	Daily Model - Annual Averages from Daily Predictions					Annual Model - Annual Predictions				
Region	**RMSE (ppb)**	**MAE (ppb)**	**Adj R^2 (ppb)**	**MB (%)**	**MAB (%)**	**RMSE (ppb)**	**MAE (ppb)**	**Adj R^2 (ppb)**	**MB (%)**	**MAB (%)**
N America	4.0	3.2	0.62	34	47	4.0	3.1	0.64	45	58
S America	3.4	2.6	0.66	28	45	4.4	3.3	0.57	1	38
Europe	4.3	3.1	0.56	17	34	4.1	2.9	0.59	16	33
Africa	3.8	2.8	0.49	22	43	3.6	2.6	0.52	16	38
Asia	4.6	3.4	0.54	17	32	4.5	3.2	0.57	17	33
Oceania	5.6	4.7	0.02	120	152	4.7	4.0	0.02	100	127
Global	4.4	3.2	0.63	21	36	4.3	3.1	0.61	22	38
Abbreviations: RMSE – root mean square error, MAE – mean absolute error, Adj R^2 – adjusted R2, MB – mean percent bias, MAB – mean absolute bias.										

Table 6 shows cross-validation model performance stratified by urbanicity (urban vs rural). RMSE is lower in rural settings vs urban settings. For example, annual RMSE is 4.6 ppb and 2.9 ppb for urban and rural air monitors, respectively. However, RMSE relative to mean concentrations are greater in rural than urban air monitors. For example, the annual mean:RMSE ratio is 2.8 and 1.8 for urban and rural air monitors, respectively.

Table 6. Cross-Validation Performance Annual LUR Model Performances Stratified by Urbanicity.

Urbanicity	**n**	**Mean (ppb)**	**RMSE (ppb)**	**Adj R^2 (ppb)**	**MB (%)**	**n**	**Mean (ppb)**	**RMSE (ppb)**	**Adj R^2 (ppb)**	**MB (%)**
Urban*	4721936	13.1	7.2	0.48	43	29956	13.1	4.6	0.65	20
Rural	992027	5.2	4.5	0.41	61	6024	5.2	2.9	0.55	27

*Includes air monitors in urban and suburban locations.

Discussion

We collected 5.7 million days of valid measurements from 8,250 air monitors and developed a daily global NO_2 model at 50 meter resolution. The model captured 47% of daily, 59% of monthly, and 63% of annual global NO_2 variation. Predictor variables for the model are available from 2005 to the

present, which allows for retrospective exposure estimates for global burden of disease studies as well as in long running epidemiological cohorts, particularly in developing countries where NO_2 data and models are limited or not available.

The model structure consists of variables with a range of spatial and temporal resolutions that correspond to NO_2 emission sources and patterns. Road networks make up variables from 50 to 200 meters in resolution. Population density and built up environment variables capture moderate spatial resolutions (2.5 and 3 km, respectively), while OMI, meteorological variables, and protective land use characteristics such as water and trees capture more regional NO_2 distributions (10 km to 31 km). While OMI and meteorological variables might have coarse spatial resolutions, these variables have daily temporal resolution and thus are responsible for the model's ability to capture day to day variation in NO_2 concentrations.

Several model variables contributed little to global variation but were highly significant to capturing regional NO_2 variation. For example, built environments explained 11.9% of NO_2 variation in Africa (specifically, South Africa), but only 1.6% of the global NO_2 variation. This highlights one of the challenges of developing large scale LUR models, in which associations between predictors and outcomes may differ when stratified by sub-regions compared to examining unstratified associations. This trade-off has been highlighted in other studies examining global NO_2 modelling [14] Other variables such as road networks may have strong associations across all subregions, but the magnitudes of those associations may differ due to regional factors such as fleet composition, traffic levels and congestion, and emission standards. In this model we included Community Emissions Data System (CEDS) [23] Sector Specific NO_x Emissions, including surface transportation emissions, but these variables were not selected in the final model.

Air monitor records are disproportionately greater in North America, Europe, and Asia. To mitigate, we weighted air monitor records to adjust for disproportionate spatial and temporal representation. Still, confidence in model predictions is greatest in these regions with greater coverage.

Regression models were fitted to minimize mean square error (MSE), the square of RMSE, and daily RMSE of continental regions with large numbers of daily records (6.4-7.3 ppb) is surprisingly greater than RMSE of regions with small numbers of daily records (5.7 to 6.7 ppb). This may be due to the higher absolute concentrations in areas where there are many monitors. In non-polluted areas with lower absolute concentrations, RMSE of ~6 ppb can still represent percent errors exceeding 100%. Despite this, for global studies which aim to standardize RMSE as equally as possible across multiple continents, the weighted modeling approach implemented in this model appears to work well. However, while RMSE is evenly distributed across regions, MB is noticeably higher and Adj. R^2 (0.10) is noticeably lower for Oceania than other regions. Poor MB and Adj. R^2 performance in Oceania is in partly attributable to the inclusion of a small set of NO_2 monitoring data from Australia that was available in OpenAQ. The mean and standard deviation of daily concentrations in Oceania is low (4 and 4 ppb, respectively) and well below global values (9 and 11 ppb). The smaller daily averages lead to larger MB when RMSE is the same. For example, an RMSE of 2 ppb with an air monitor record of 2 ppb is a 100% MB, while an RMSE of 2 ppb with an actual concentration of 20 ppb is 10% MB.

In our sensitivity analysis we used our data to develop new monthly and annual NO_2 models and compared these model cross-validation performances to monthly and annual averages of the daily model predictions. Differences between models were within 2%, which is within the random variation observed between bootstrap cross-validation instances. The geographic variables includes in the monthly and annual model (Table S4) were similar to the daily model, suggesting these are consistently the most important predictors of geographical NO_2 patterns. These comparisons suggest using the daily model for deriving monthly and annual exposures does not increase model error. However, it also suggests the additional computational costs of deriving daily results is not needed unless health studies can leverage daily exposure estimates to refine their health analyses. For acute studies such as hospital admissions following extreme exposures, daily estimates can be more useful than monthly or annual estimates.

Sensitivity models suggest model performance differs between urban and rural areas. Model predictions for rural locations have greater error than their respective urban counterparts, which is not surprising given the limited number of rural air pollution monitors available. For studies with rural participants, we recommend either using annual rather than daily or monthly model predictions or restricting analyses to urban and suburban participants.

Our NO_2 model has several limitations that should be considered when applying the model. First, model predictions are dependent on valid daily OMI measurements. In addition to meteorological limitations such as cloud cover, the number of valid daily pixel measurements from the OMI sensor on the Aura satellite has gradually been decreasing over time due to an instrument obstruction first noticed in 2007 [24]. From 2018 onwards, measurements are available from the TROPOMI instrument, with substantially higher spatial resolution compared with OMI. Future studies would benefit from an adaptation of this model using TROPOMI rather than OMI as the satellite-based measure of columnar NO_2. Second, this model relies on road networks as a secondary indicator for vehicle emissions. Travel patterns have significantly changed since the onset of the COVID-19 pandemic and studies have demonstrated significant declines in NO_2 during lock-down periods [25]. We therefore restricted our model training and performance analysis to the years 2005 to 2019. Future research should examine potential long-term changes in travel behavior and how this impacts NO_2 levels and patterns.

We created a daily global NO_2 model with 50m spatial resolution, with coverage from 2005-2019. In bootstrap cross-validation, the model captured 47%, 59%, and 63% of daily, monthly, and annual variation in NO_2 concentrations. We will make these NO_2 model estimates available, which can be used to retrospectively estimate acute and chronic exposures for risk assessments (e.g. global burden of disease studies), for multi-national health studies, where measurements are ideally standardized across regions, and for studies in developing countries were NO_2 monitoring data or detailed models are not available.

Funding Sources:

This study was supported by grants from the Health Effects Institute and Bloomberg Philanthropies (research agreement 4977/20–11).

References:

[1] Cohen AJ, et al. Estimates and 25-year trends of the global burden of disease attributable to ambient air pollution: an analysis of data from the Global Burden of Diseases Study 2015. The Lancet. 2017;389(10082):1907-1918.

[2] Beckerman B, Jerrett M, Brook JR, Verma DK, Arian MA, Finkelstein MM. Correlation of nitrogen dioxide with other traffic pollutants near a major expressway. Atmos Environ. 2008;42(2):275–290. 5.

[3] Khreis H, Kelly C, Tate J, Parslow R, Lucas K, Nieuwenhujisen M. Exposure to traffic-related air pollution and risk development of childhood asthma: A systematic review and meta-analysis. Environ Int. 2017;100:1–31.

[4] Wang Z, et al. Association between short-term exposure to air pollution and ischemic stroke onset: a time-stratified case-crossover analysis using a distributed lag nonlinear model in Shenzhen, China. Environ. Health. 2020;19.(1): 1-12.

[5] Rice MB, Ljungman PL, Wilker EH, Gold DR, Schwartz JD, Koutrakis P, Washko GR, O'Connor GT, Mittleman MA. Short-term exposure to air pollution and lung function in the Framingham Heart Study. Am J Respir Crit Care Med. 2013;188(11):1351–1357.

[6] Hamra GB, Laden F, Cohen AJ, Raasachou-Nielsen O, Brauer M, Loomis D. Lung cancer and exposure to nitrogen dioxide and traffic. Environ Health Perspect. 2015;123(11):1107–1112.

[7] VanGeffen J, Eskes HJ, Boersma KF, Maasakkers JD, Veefkind JP. TROPOMI ATBD of the Total and Tropospheric NO2 Data Products. 2021.

[8] Levelt, P et al. The Ozone Monitoring Instrument: Overview of 14 Years in Space. Atmos. Chem. Phys. 2018;18(8):5699–5745. https://doi.org/10.5194/acp-18-5699-2018.

[9] Krotkov NA et al. Aura OMI Observations of Regional SO2 and NO2 Pollution Changes from 2005 to 2015. Atmos. Chem. Phys. 2016;16(7):4605–4629. https://doi.org/10.5194/acp-16-4605-2016.

[10] Duncan BN, Lamsal LN, Thompson AM, Yoshida Y, Lu Z, Streets DG, Hurwitz MM, Pickering KEA. Space-Based, High-Resolution View of Notable Changes in Urban NOx Pollution around the World (2005-2014). J. Geophys. Res. Atmos. 2016;121(2):976–996. https://doi.org/10.1002/2015JD024121.

[11] Jamali S, Klingmyr D, Tagesson T. Global-Scale Patterns and Trends in Tropospheric NO2 Concentrations, 2005-2018. Remote Sens. 2020;12:(21):3526. https://doi.org/10.3390/rs12213526.

[12] Sun K, et al. A Physics-Based Approach to Oversample Multi-Satellite, Multi-Species Observations to a Common Grid. Atmos. Meas. Tech. Discuss. 2018;11:(12):1–30. https://doi.org/10.5194/amt-2018-253.

[13] Goldberg DL, Anenberg SC, Kerr GH, Mohegh A, Lu Z, Streets DG. TROPOMI NO2 in the United States: A Detailed Look at the Annual Averages, Weekly Cycles, Effects of Temperature, and Correlation With Surface NO2 Concentrations. Earth's Futur. 2021;9(4), e2020EF001665. https://doi.org/10.1029/2020EF001665.

[14] Larkin A, et al. Global land use regression model for nitrogen dioxide air pollution. Environ. Sci. & Technol. 2017;51(12):6957-6964.

[15] Lu M, et al. Evaluation of different methods and data sources to optimise modelling of NO2 at a global scale. Environ. International. 2020;142:105856.

[16] Cooper MJ, et al. Inferring ground-level nitrogen dioxide concentrations at fine spatial resolution applied to the TROPOMI satellite instrument. Environ. Research Letters. 2020;15(10):104013.

[17] Yin P, et al. The effect of air pollution on deaths, disease burden, and life expectancy across China and its provinces, 1990–2017: an analysis for the Global Burden of Disease Study 2017. The Lancet Planetary Health. 2020;4(9):e386-e398.

[18] Dunlea EJ, et al. Evaluation of Nitrogen Dioxide Chemiluminescence Monitors in a Polluted Urban Environment. Atmos. Chem. Phys. 2007;7(10):2691–2704. https://doi.org/10.5194/acp-7-2691-2007.

[19] Dickerson RR, Anderson DC, Ren X. On the Use of Data from Commercial NOx Analyzers for Air Pollution Studies. Atmos. Environ. 2019;116873. https://doi.org/10.1016/j.atmosenv.2019.116873.

[20] Lamsal LN., et al. Ozone Monitoring Instrument (OMI) Aura nitrogen dioxide standard product version 4.0 with improved surface and cloud treatments. Atmospheric Measurement Techniques. 2021;14(1):455-479.

[21] Corbane C, Florczyk A, Pesaresi M, Politis P, Syrris V. GHS built-up grid, derived from Landsat, multitemporal (1975-1990-2000-2014), R2018A. European Commission, Joint Research Centre (JRC). 2018. https://doi.org/10.2905/jrc-ghsl-10007.

[22] Vohra Karn, et al. Long-term trends in air quality in major cities in the UK and India: a view from space. Atm. Chem. and Physics. 2011;21(8):6275-6296.

[23] McDuffie EE, et al. A global anthropogenic emission inventory of atmospheric pollutants from sector-and fuel-specific sources (1970–2017): an application of the Community Emissions Data System (CEDS). Earth System Science Data. 2020;12(4):3413-3442.

[24] Schenkeveld VM, et al. In-flight performance of the Ozone Monitoring Instrument. Atmospheric measurement techniques. 2017;10(5):1957-1986.

[25] Hoang AT, et al. An analysis and review on the global NO2 emission during lockdowns in COVID-19 period. Energy Sources, Part A: Recovery, Utilization, and Environmental Effects. 2021;1-21.

Supplemental Materials.

Table S1. Air Monitor Record Data Sources.

Data Source	Monitors (n)	Daily* (n)	Temporal Coverage*	Spatial Coverage	Website
OpenAQ	6134	3300710	2015-2019	Global	openaq.org
NAPS	262	767525	2005-2018	Canada	www.canada.ca/en/environment-climate-change/services/air-p data/national-air-pollution-program.html
US EPA	801	2084273	2005-2019	US	aqs.epa.gov/aqsweb/documents/data_mart_welcome.html
EU Airbase	4975	7235828	2012-2019	Europe	www.eea.europa.eu/data-and-maps/data/airbase-the-european
Japan Ministry of the Environment	912	2642571	2009-2017	Japan	www.env.go.jp/en/air/aq/aq.html
SAAQIS	90	115363	2005-2019	South Africa	saaqis.environment.gov.za/
Mexico Ministry of the Environment	62	136589	2005-2019	Mexico	www.aire.cdmx.gob.mx/default.php

*Number of valid daily averages. Abbreviations: AQ – Air Quality, NAPS – National Air Pollution Surveillance Program, US EPA – United States Environmental Protection Agency, EU: European Union, SAAQIS: South African Air Quality Information System. *Air monitor records preceding 2005 were not collected.

Table S2. Predictor Variable Buffer Distances.

Buffer Distances (m)									
50	100	200	300	400	500	600	700	800	1000
1200	1500	2000	2500	3000	3500	4000	5000	6000	7000
8000	10000	15000	20000						

Table S3. Sectors Included in CEDS Emission Estimates.

Sector	Description
AGR	Non-combustion agricultural sector
ENE	Energy transformation and extraction
IND	Industrial combustion and processes
TRA	Surface Transportation (Road, Rail, Other)
RCO	Residential, commercial, and other
SLV	Solvents
WST	Waste disposal and handling
SHP	International shipping (including VOCS from oil tanker loading/leakage)

Table S4. Comparison of Variables Selected by Lasso to Predict Daily, Monthly, or Annual Air Monitor Averages

	Daily	Monthly	Annual
Major Roads	x	x	x
OMI	x	x	x
Built Environment	x	x	x
Population Density	x		x
Tree Cover	x		
Minor Roads	x		x
Residential Roads	x	x	x
Water Body	x		
Temperature	x		x
Atm Pressure	x	x	x
Solar Radiation		x	x
Precipitation		x	x
Elevation		x	
Railways			x

Table S5. NO_2 Model Training Performance.

	Daily					Monthly					Annual				
Region	**RMSE (ppb)**	**MAE (ppb)**	**Adj R^2 (ppb)**	**MB (%)**	**MAB (%)**	**RMSE (ppb)**	**MAE (ppb)**	**Adj R^2 (ppb)**	**MB (%)**	**MAB (%)**	**RMSE (ppb)**	**MAE (ppb)**	**Adj R^2 (ppb)**	**MB (%)**	**MAB (%)**
N America	6.4	4.8	0.51	57	80	4.9	3.9	0.54	49	63	4.0	3.2	0.62	34	47
S America	6.2	4.4	0.37	55	78	4.4	3.4	0.50	37	59	3.4	2.6	0.66	28	45
Europe	6.4	4.6	0.45	39	63	4.8	3.5	0.53	26	44	4.3	3.1	0.56	17	34
Africa	6.7	4.3	0.35	54	80	5.1	3.1	0.39	23	48	3.8	2.8	0.49	22	43
Asia	7.3	5.4	0.40	45	65	5.2	3.8	0.53	24	40	4.6	3.4	0.54	17	32
Oceania	5.7	4.5	0.10	168	187	5.5	4.8	0.10	164	185	5.6	4.7	0.02	120	152
Global	6.8	5.0	0.47	46	68	5.0	3.7	0.59	30	46	4.4	3.2	0.63	21	36

Abbreviations: RMSE – root mean square error, MAE – mean absolute error, Adj R^2 – adjusted R2, MB – mean percent bias, MAB – mean absolute bias.

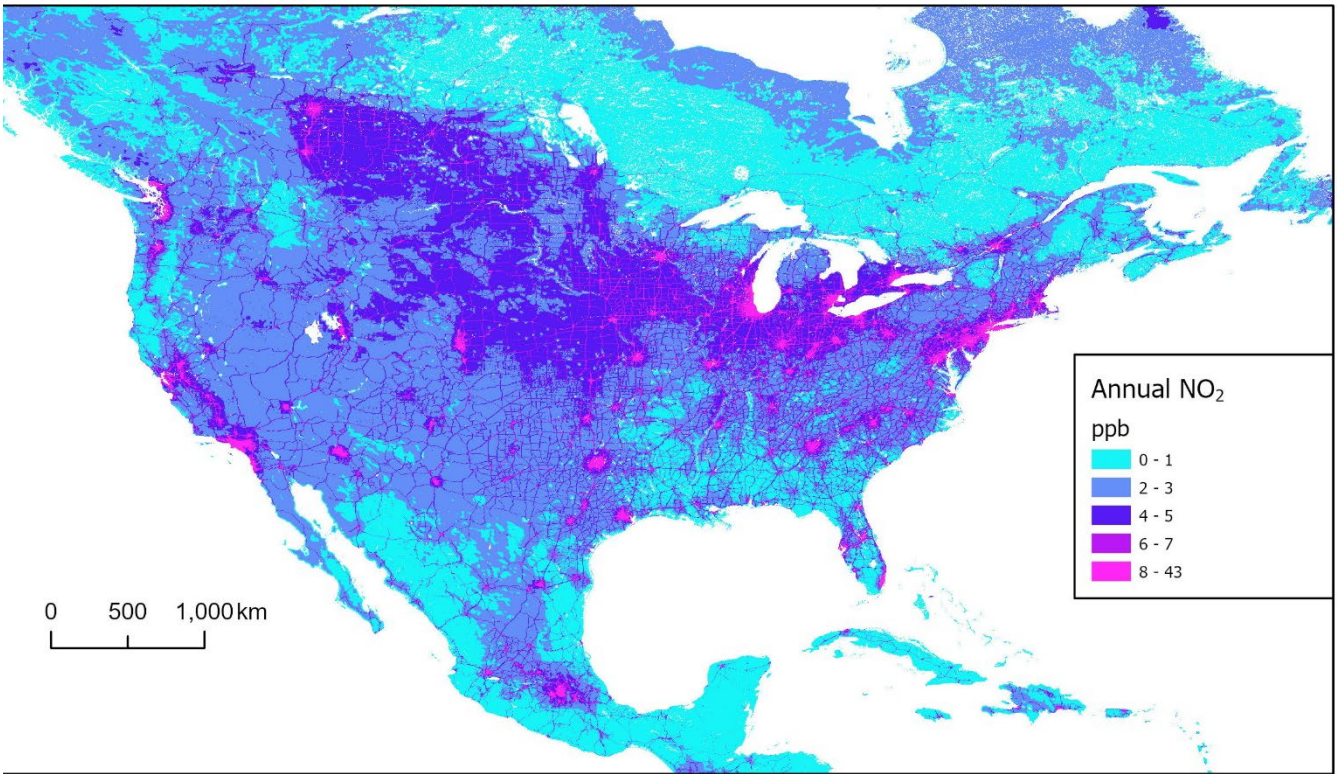

Figure S1. Distribution of Annual 2018 NO_2 Concentrations Across Mexico, Southern Canada, and the Continental US. The color ramp was chosen to emphasize the distribution of annual concentrations below 5ppb.

Figure S1. Geographic Weighting.

Define the variable s_h as follows:

$$s_h = \frac{n * N_h * \sigma_h}{\sum_{k=1}^{L} N_k * \sigma_k}$$

Where

s_h = number of units sampled from region h

n = total number of units sampled

σ_h = standard deviation of region h

σ_k = standard deviation of region k

N_h= number of units available from region h

N_k= number of units available from region k

L= number of regions

Let the geographical weights for regions be defined as follows

$$g_h = \frac{s_h}{n_h}$$

Where

g_h = weight for each annual monitor in region h

s_h = number of units sampled from region h

n_h = number of annual monitors in region h

Let the geographical and monthly weights for each region-month be defined as follows

$$g_{hi} = \frac{s_h}{12 * n_{hi}}$$

Where

g_{hi} = weight for each daily air monitor in region h and month i

s_h = number of units sampled from region h

n_{hi} = number of daily air monitors in region h and month i